Tailoring the Trajectory of Cell Rolling with Cytotactic Surfaces

ARTICLE *in* LANGMUIR · NOVEMBER 2011

Impact Factor: 4.46 · DOI: 10.1021/la203382k · Source: PubMed

Langmuir

ARTICLE

pubs.acs.org/Langmuir

Tailoring the Trajectory of Cell Rolling with Cytotactic Surfaces

Collin Edington,[†,§] Hironobu Murata,[§] Richard Koepsel,[§,∥] Jill Andersen,[§] Sungeun Eom,[⊥] Takeo Kanade,[⊥] Anna C. Balazs,[‡] German Kolmakov,[‡] Carsen Kline,[#] Daniel McKeel,[§] Zvi Liron,[▽] and Alan J. Russell*[,§,∥]

[†]Department of Bioengineering, [‡]Department of Chemical Engineering, and [§]McGowan Institute for Regenerative Medicine, University of Pittsburgh, Pittsburgh, Pennsylvania, United States

[∥]Department of Surgery, University of Pittsburgh Medical Center, Pittsburgh, Pennsylvania, United States

[⊥]Robotics Institute and [#]Electrical and Computer Engineering, Carnegie Mellon University, Pittsburgh, Pennsylvania, United States

[▽]Department of Physical Chemistry, Israel Institute for Biological Research, Ness-Ziona, 74100, Israel

Supporting Information

ABSTRACT: Cell separation technology is a key tool for biological studies and medical diagnostics that relies primarily on chemical labeling to identify particular phenotypes. An emergent method of sorting cells based on differential rolling on chemically patterned substrates holds potential benefits over existing technologies, but the underlying mechanisms being exploited are not well characterized. In order to better understand cell rolling on complex surfaces, a microfluidic device with chemically patterned stripes of the cell adhesion molecule P-selectin was designed. The behavior of HL-60 cells rolling under flow was analyzed using a high-resolution visual tracking system. This behavior was then correlated to a number of established predictive models. The combination of computational modeling and widely available fabrication techniques described herein represents a crucial step toward the successful development of continuous, label-free methods of cell separation based on rolling adhesion.

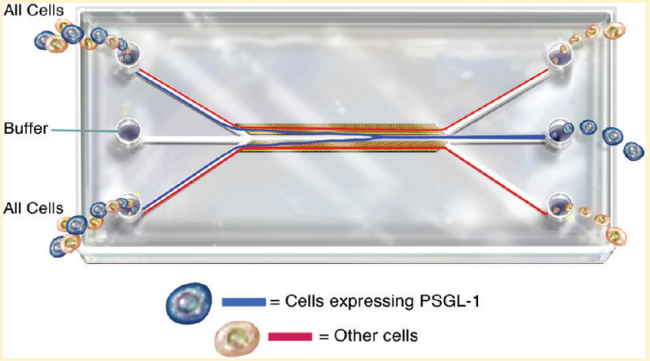

INTRODUCTION

The ability to separate specific populations of cells from a heterogeneous sample is a fundamental requirement for studying cell biology. Medical diagnostics and cell-based therapies also rely on cell separation technologies to ensure safe and effective treatment. Since the 1970s, fluorescent activated cell sorting (FACS) has been the workhorse of cell separation techniques due to the high specificity, rapid separation, and wide range of commercially available fluorescent markers.[1,2] While FACS has evolved considerably over the past 40 years to increase specificity, efficiency, and speed, it still remains an expensive and often time-consuming process that relies on covalently bound or antibody conjugated markers to identify specific cell populations. As a result, the technique is not ideal for sensitive cell populations or applications where cell phenotype must be preserved. The additional cost and complexity of cell labeling also limits the use of FACS and similar techniques in point-of-care diagnostics. The limitations of label-based cell separation techniques have inspired the development of numerous label-free methods, many of which are based on microfluidic manipulation of cell solutions. These methods rely primarily on physical properties, such as dielectric charge, cell size, and autofluorescence to separate different populations.[3−9] However, many cell phenotypes are exclusively defined by their expression of specific membrane proteins, rather than electrical or mechanical properties. There exists a need for a device capable of continuous, label-free separation of cells based on the expression of surface proteins.

By rationally tailoring the microenvironment of a cell, it may be possible to manipulate and characterize the cell without attaching ligands to its surface. As cells pass over surfaces, there is an opportunity to deliver signals to the cell from the surface that cause the cell to alter its behavior. Surfaces that can deliver a stimulus that directs cells toward or away from the surface are known as cytotactic surfaces. Indeed, in biology, such surfaces already exist. Following tissue injury, one of the earliest steps of the inflammatory response is the recruitment of white blood cells (leukocytes) from nearby vasculature. Leukocyte extravasation is initiated by the expression of cell adhesion molecules, including E- and P-selectin, on the surface of activated endothelial cells, which causes free floating leukocytes expressing P-selectin Glycoprotein Ligand-1 (PSGL-1) to adhere to the vessel walls and roll to the site of injury before escaping the blood vessel.[10] Selectin mediated rolling has been studied extensively,[10−22] and a number of attempts have been made to purify hematopoietic cells based on this unique interaction.[23−25] Some of these methods are based on

Received: August 29, 2011
Revised: October 25, 2011

   dx.doi.org/10.1021/la203382k | *Langmuir* XXXX, XXX, 000–000

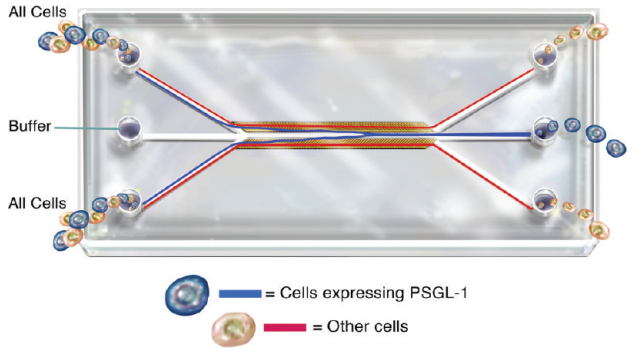

Figure 1. Artistic rendition of the microfluidic device used in this study. The device was designed with the capability to sort cells using patterned stripes of P-selectin, although sorting effectiveness has not yet been studied. Angled stripes on either side of the channel direct rolling cells (blue) toward the center pathway where they are collected as they exit the device. Cells that do not interact with the surface or do not express P-selectin glycoprotein ligand-1 (red) follow the direction of flow and exit through the two side channels.

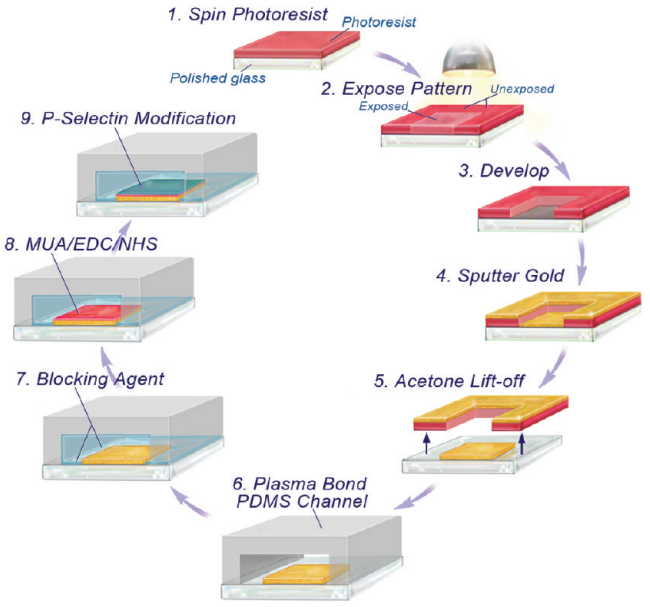

Figure 2. Overview of the process for fabricating the microfluidic cell sorter shown in Figure 1. Striped patterns are achieved by depositing gold using sputtering and a negative photoresist lift-off technique. Oxygen plasma bonding is then used to seal a PDMS channel to the glass substrate. After applying a fluorinated agent to block nonspecific interactions, P-selectin is covalently attached to the gold stripes.[31]

differential rolling adhesion in one dimension or static adhesion, but they are not continuous and require careful collection of samples at specified time points.

A recent computational model reveals an improved method of adhesion-based separation by incorporating arrays of chemically and mechanically patterned surface features.[26] The model suggests that passive, label-free cell separation could be accomplished in a microfluidic package by utilizing smart surfaces to identify differences in cell surface ligands or cell membrane stiffness. The virtual surface utilizes angled stripes of variable stiffness or adhesiveness. As "cells" roll along the virtual surface under laminar flow, they can obtain a net displacement perpendicular to the direction of flow upon interacting with a diagonal stripe that has a higher adhesive interaction or lower modulus than the bulk material. This predicted displacement results from a change in shear forces as laminar flow pushes the capsule across each stripe, and is also a function of the capsule's stiffness, meaning that two capsules with different compliances or adhesive properties will exhibit different amounts of displacement, effectively sorting them. The capsule's path is altered as it passes from the weakly adhesive bulk material to the "sticky" stripe, and after exposure to multiple stripes the compliant capsules gain displacement perpendicular to the direction of flow.

Control of cell motion in two dimensions would allow for the physical segregation of interacting and noninteracting cells in a continuous manner, making such a sorting method attractive. Consequently, experimentally verifying and understanding this prediction is an important step toward the practical development of an adhesion-based sorting device. Results from experimental manipulations of leukocytes appear to support the Balazs model, including the observation of lateral displacement on stripes of P-selectin and the absence of the effect in the case of rigid microspheres.[27,28] Only the macroscopic behavior of cells in these systems has been investigated, and therefore, the data lack the necessary resolution to verify the model. In order to more fully understand cellular motion across patterned surfaces, we developed a system in which we could observe these interactions on a submicrometer scale. A mechanistic understanding of this effect would be important in the successful development of adhesion-based methods of cell sorting.

We designed a microfluidic device to study the directed rolling of cells using a cytotactic surface of covalently immobilized P-selectin. We patterned this surface to the dimensions outlined in the Balazs model and observed the response of rolling HL-60 cells.[29] HL-60 cells are a human myeloid cell line expressing high levels of PSGL-1 that are commonly used in leukocyte rolling experiments.[10,12,27,29,30] The paths of the cells were recorded using a customized MATLAB tracking program and compared to the theoretical response predicted by the model. The device represents a foundation that can be adapted to any transiently binding cell/ligand combination. With improvements in micropatterning technology, cytotactic microfluidic devices could be designed to screen for the presence of many different surface markers simultaneously, without the obligatory attachment of a potentially disruptive chemical tag to the cell. For the scope of this study, however, we are concerned primarily with characterizing the specific response of HL-60 cells to patterned stripes of P-selectin. The philosophy of this approach is outlined in Figure 1.

MATERIALS AND METHODS

Synthesis and Fabrication of a Rationally Designed Cytotactic Surface. To generate a surface that could influence the direction in which cells rolled over it, we selected a foundation layer of glass upon which we could fabricate the necessary synthetic elements. Using the Balazs/Alexeev model to define the geometry, we designed a network of gold stripes on glass slides. Gold stripes were chosen in lieu of microcontact printing because they provided a substrate for the covalent immobilization of the P-selectin and provided greater visual contrast for image tracking purposes.[28,31] The stripes were arranged in two rows along the sides of the fluid channel, with an unpatterned region in the middle. The individual stripes were 5 μm wide with a space of 10 μm between each stripe and were angled at 45° with respect to the direction of flow in order to direct cells toward the center channel. A diagram of the fabrication procedure is shown in Figure 2.

dx.doi.org/10.1021/la203382k |*Langmuir* XXXX, XXX, 000–000

A 4 in. polished glass wafer was patterned using image reversal of AZ5214-E photoresist (Microchemicals Inc.) and a bright field chrome photomask of the stripe pattern (Photo Sciences Inc.). A sputtered titanium underlayer (5 nm) was subsequently coated with sputtered gold (20 nm), and the gold-striped glass wafer was then diced into individual units that would form the bottoms of the flow chambers. The quality of the patterned surface was characterized by scanning electron microscopy (SEM, FEI Sirion).

The sidewalls and ceiling of the fluid channels (1.2 mm wide by 10 mm long) were made from poly(dimethyl siloxane) (PDMS). A silicon mold for the PDMS top layer was prepared by traditional lithographic techniques and anisotropic reactive ion etching to a depth of 30 μm. After etching, the wafers were cleaned and treated with trichloro(1,1,2,2 perfluorooctyl)silane vapor to facilitate PDMS release from the mold. The polymer was made using a SYLGARD 184 silicone elastomer kit (Dow Corning Corporation). After combining the base and curing agent (10:1), the mixture was degassed under vacuum for 45 min. Degassed PDMS was poured evenly over the mold and allowed to cure overnight at room temperature, and then it was baked at 70 °C for 1 h. After curing, the PDMS was cut into individual units and holes were punched at the inlets and outlets.

In order to achieve a strong mechanical seal and prevent leaks between the cytotactic surface and the chamber walls, the PDMS and glass were bonded using an oxygen plasma treatment.[32,33] The layers were activated in a plasma barrel etcher (International Plasma Corporation, O_2 plasma, 18 s, 50 W, 1 Torr). Following plasma activation, the layers were heated to 75 °C for 5 min. They were then mounted in a Karl Süss MJB3 Contact Aligner and brought into light contact to initiate bonding.

A rational design of the cytotactic surface requires that the nonbiologically active part of the surface is inert. We therefore "blocked" the glass surface within 1 h of plasma treatment using a 1% solution of (heptadecafluoro-1,1,2,2-tetrahydrodecyl)dimethyl-chlorosilane (Gelest, Inc.) in filtered acetonitrile. A micropipet was used to inject 10 μL of blocking solution into the sealed chambers. After incubation at room temperature for 1 h, chambers were rinsed repeatedly with acetonitrile and dried with nitrogen.

Our next step was to introduce the cytotactic element onto the gold stripes by chemical modification.[31] A 11-mercaptoundecanoic acid (MUA) solution was prepared by combining MUA (11 mg), pure ethanol (10 mL), and HCl (50 μL). The solution was then filtered with a PTFE syringe filter and infused with argon gas for 10 min. MUA solution (10 μL) was injected into the flow chambers and the tray holding the chambers was charged with argon and sealed. After incubation for 1 h at room temperature, the flow chambers were washed three times with ethanol and dried with nitrogen.

To prepare the MUA-modified gold stripes for attachment to a biomolecule, an EDC-NHS solution was prepared by combining *N*-(3-dimethylaminopropyl)-*N*′-ethylcarbodiimide hydrochloride (EDC, 20 mg) with *N*-hydroxysuccinimide (NHS, 12 mg) in acetonitrile (10 mL). The EDC-NHS solution (10 μL) was injected into the chambers using a micropipet. After incubating for 30 min at room temperature, the chambers were washed with acetonitrile and dried with nitrogen.

Finally a P-selectin solution was prepared by combining P-selectin stock solution (ADP3-200, R&D Systems, 10 μL of 200 μg/mL) with filtered Dulbecco's phosphate buffered saline (DPBS, Fischer-Scientific BW17-512F, 90 μL) for a final concentration of 20 μg/mL of P-selectin. The chambers were injected with P-selectin (10 μL) solution and incubated for 1 h at room temperature. After incubation the chambers were rinsed repeatedly with DPBS and dried with nitrogen. After P-selectin modification, chambers were stored at 4 °C until use.

P-Selectin site density was determined using mouse anti-human P-selectin (R&D Systems, ADP3) followed by goat anti-mouse IgG-HRP (R&D Systems, HAF007) and a spectrophotometric assay. P-Selectin density was determined to be 1300 molecules/μm^2. Additionally, the stability of P-selectin on gold-coated surfaces was tested in dry and wet (PBS) conditions. P-Selectin activity decreased after 32 days of storage (4 °C) in dry and wet conditions by 25% and 70%, respectively.

P-Selectin modification was verified by labeling with fluorescent polystyrene microbeads (0.5 μm diameter, Invitrogen F-8813) that were functionalized with human P-selectin mAb (R&D Systems, BBA30). Briefly, carboxylate modified polystyrene microspheres were incubated in a solution of EDC·HCl (4 mg), NHS (2.2 mg) and DI water (1 mL) for 30 min. After rinsing with DI water, the microspheres were then incubated with human P-selectin mAb (100 μg/mL) reconstituted in phosphate buffer (10 mM, pH 8.5) for 1 h before being washed with DPBS. A 1:9 solution of microspheres (15 mg/mL) and DPBS was injected into the flow chambers and incubated at room temperature for 1 h and then rinsed with DPBS and dried with nitrogen. Fluorescence imaging was used to visualize the quality of the chemical modification.

Tracking and Analysis of HL-60 Cell Rolling on a Patterned Surface. Human leukocyte cells (HL-60, ATCC #CCL-240) were cultured in polystyrene tissue culture flasks (DB Falcon, 75 cm^2) under recommended ATCC conditions (37 °C, 5% CO_2) with a growth medium consisting of ATCC-formulated Isocove's modified Dulbecco's medium with 20% fetal bovine serum. Cell concentration was maintained between 10^5-10^6 cells/mL.

Flow experiments were performed using a solution of PBS with 1 mM $CaCl_2$ and 1 mM $MgCl_2$. Consistent flow rates were achieved using a Harvard Apparatus PHD2000 infuser with three microsyringes (Hamilton Co. GASTIGHT #1802). In parallel with the microsyringes was a microinjector (Narishige, IM-9A) for manual infusion, flushing of the chambers, and introduction of cells. After priming the system with liquid, a small volume of cells (10−15 μL) was introduced to the lower inlet tube at a concentration of 1×10^5 cells/mL.

Images and videos were acquired using a Leica DM-IRB inverted microscope (40× objective), Leica DFC480 C-mount 5 megapixel camera, and Leica Application Suite (Ver. 3.3.0). A range of flow rates from 0.03 to 0.24 μL/min were evaluated. Fluid velocities and shear stress were calculated for each flow rate.[34]

Tracking data were acquired from the recorded video segments using custom, GUI-based MATLAB tracking software. The software estimates the background and subtracts it from each frame. Then, ring shaped templates of different sizes (Laplacian filters of varying standard deviation) are applied to the subtracted image to identify cells. A one-to-one assignment algorithm is then used to connect the detected cells across multiple frames for continuous tracking.

Before tracking, the software located the edges of the stripes to allow analysis of cell motion at four different regions: within stripes, within gaps, in the gap-to-stripe transition region, and in the stripe-to-gap transition region. Measuring motion in each of these regions provided the necessary resolution to compare experimental data to the model predictions. The necessary factor to convert pixels to distance was determined to be 0.5 μm/pixel. The frame rate was 10.0 frames per second and was verified with a recording of a timed LED circuit board.

RESULTS

Synthesis and Fabrication of a Rationally Designed Cytotactic Surface. The Balazs model predicts that a glass surface with an appropriate array of bioactive stripes would alter the trajectory of cells rolling over it. As described above, we used sputtered gold deposition and custom designed masks to deposit a foundation for the attachment of a bioactive molecule. The physical dimensions of the resultant stripes were measured using a mechanical stylus profilometer. Stripe width was 6.6 ± 0.2 μm,

dx.doi.org/10.1021/la203382k |*Langmuir* XXXX, XXX, 000–000

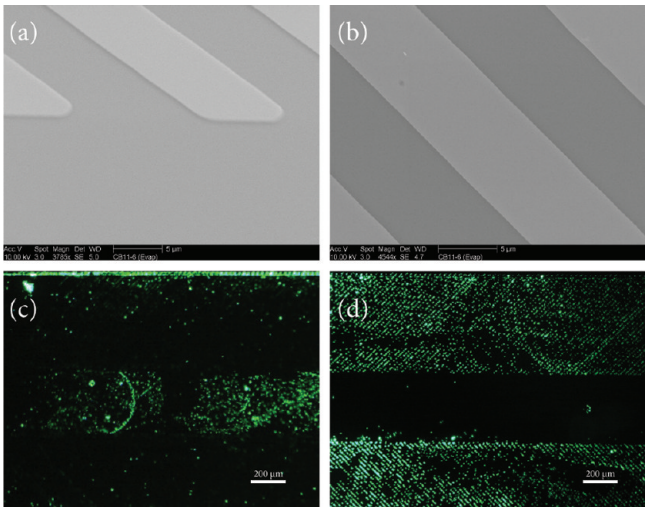

Figure 3. Characterization of the physical and chemical patterning of the cytotactic surface. Scanning electron microscopy (a,b) shows that the stripes are patterned at a high resolution with well-defined edges. Control chambers (c) exhibit high amounts of nonspecific binding in the central channel. Chambers modified with blocking agent and P-selectin (d) demonstrated a significant reduction in nonspecific binding and visible patterning of the fluorescent microspheres, indicating that P-selectin was confined to the gold stripes.

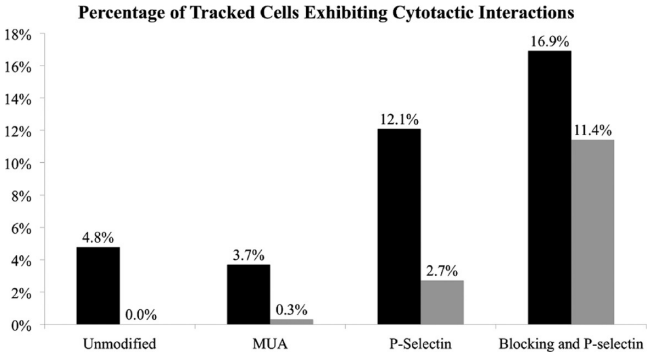

Figure 4. Percentage of cells exhibiting cytotactic behavior, defined as a velocity below 50% of the hydrodynamic velocity, without being influenced by the path of another cell. Cells undergoing permanent adhesion were not included, as their paths could not be analyzed. Percentages are averaged over all flow rates, as no significant differences were observed between different flow rates. Because many of the interacting cells only appeared to interact with a single stripe before detaching and becoming free-flowing, we also classified the subset of cells that interacted multiple times. The percentage of total cells exhibiting behavior indicative of a cytotactic interaction (black) was higher in chambers modified with P-selectin. Chambers with blocking agent showed an increased likelihood of repeated interactions (gray). Almost no instances of interactions were observed on chambers without P-selectin. (N = 3477 cells).

spacing between stripes was 8.0 ± 0.1 μm, and vertical thickness of the gold was approximately 29 nm. Scanning electron microscopy was used to visualize the profile of the stripes and verify the accuracy of the gold patterning.

The glass surfaces were then bonded to PDMS channels using oxygen plasma as described above. Plasma bonding was performed prior to chemical immobilization of P-selectin to avoid the harmful effects of high-energy plasma on the deposited protein, and to ensure a strong, continuous seal around the channels and inlets. Once the sealed chamber was established, the blocking agent was applied through the inlet ports, followed by the chemical species necessary to immobilize P-selectin to the gold stripes. To examine the effectiveness of chemical patterning, fluorescent polystyrene microspheres conjugated with anti-P-selectin mAb were exposed in flow to the surface. The data reveal that P-selectin was immobilized almost exclusively on the striped regions, with minimal nonspecific binding when the blocking agent had been applied (Figure 3). Flow chambers without blocking agent showed much less contrast between stripes and bulk material.

Tracking and Analysis of HL-60 Cell Rolling on Patterned Surfaces. Previous studies in cell rolling have either normalized velocity for all cells or used velocity changes to differentiate between floating and rolling cells.[19,28] In order to study individual interactions, however, a more precise approach was necessary. First, cells exhibiting velocities below 50% of the hydrodynamic velocity were identified using the tracking data. Cell paths were then manually examined for irregularities that might inhibit analysis. Any cells exhibiting permanent adhesion or paths perturbed by other cells were excluded. Cells exhibiting velocities consistent with the predicted hydrodynamic velocity were assumed to be noninteracting and were also excluded.

The fraction of all cells exhibiting cytotactic interactions reaches a maximum when blocking agent and P-selectin are used concurrently (Figure 4). Cells interacting with multiple stripes were not observed in control chambers without P-selectin, and a higher frequency of stripe interactions was observed when blocking agent was used. Flow rate (within the range tested) did not have any significant effect on the frequency of interactions observed. The fraction of cells exhibiting permanent adhesion was about 23% in the blocking+P-selectin experiments.

Detachment of HL-60 cells from P-selectin surfaces has been shown to be a random, history independent process that occurs when new adhesive bonds fail to form.[28] As a result, it can be difficult to determine precisely when and where a cell detaches from the surface, and behavior across any single stripe may not effectively capture the complete interaction. Therefore, we isolated paths in which cells interacted with at least three consecutive stripes, and averaged their motion over those specific stripes. An example of a cell exhibiting multiple interactions is shown in Figure 5a. An averaged path of multiple interacting cells is shown below exhibiting an average displacement of approximately 10% (Figure 5c, n = 6 cells). The same form of analysis is shown for noninteracting cells from the same video file, demonstrating an absence of lateral displacement (Figure 5b/d, n = 9 cells). For each cell included in Figure 5, the net vertical displacement was calculated as the difference between the starting and ending positions. An independent means t test revealed that the average displacement of the interacting cells (27.3 ± 8.8 μm) was significantly different (p = 0.001) from that of the noninteracting cells (2.7 ± 2.8 μm). The slight positive displacement of the interacting cells can easily be attributed to the marginal error of aligning the chambers manually under the microscope. Assuming that the slope of the chamber introduces an artificial displacement of ~2.7 μm across the field of view (~500 μm), we can estimate the actual displacement to be approximately 25 μm, or 5% displacement.

DISCUSSION

The design of the microfluidic device was driven by a desire to observe, at high resolution, how cell motion is impacted by patterned

dx.doi.org/10.1021/la203382k |*Langmuir* XXXX, XXX, 000–000

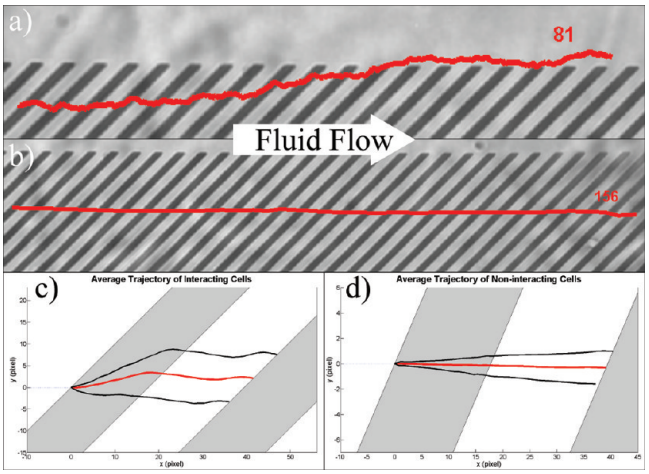

Figure 5. Behaviors of interacting and noninteracting cells were visibly different. A representative path of an interacting cell (a) and a non-interacting cell (b) are magnified to demonstrate the rolling behavior and direction of fluid flow (left to right), respectively. By combining the paths of multiple cells from a single video file, the average path they take over a single stripe can be plotted. The mean of this path is shown in red, with black lines representing one standard deviation from the mean. Average paths for interacting (c) and noninteracting (d) cells are shown ((c) $n = 6$ cells, 92 data points; (d) $n = 9$ cells, 96 data points).

surfaces. The data clearly demonstrated that not only do the average paths of interacting cells differ from those of noninteracting cells, but more importantly cell motion *entering, on, and leaving* the patterned stripes bore remarkable similarities to the motions predicted by the Balazs model. The Balazs model predicts an initial downward motion as the cell enters an adhesive stripe. The path of cell #81 (expanded in Figure 5) provides a compelling example of such behavior in our microfluidic device. The repetition of this behavior on the same length scale as the stripes further verifies the successful patterning of the surface and the interaction of the cells with that surface.

The Balazs model next predicts a change in direction as the cell becomes localized within the stripe. Because the system was designed at sufficient resolution, we were able to observe this transition experimentally in almost every case where a cell was shown to be interacting with the surface. The final element of the Balazs model predicts the path that a cell would take as it exits an adhesive stripe. As shown in Figure 5, the data fit the model.

In addition to demonstrating the existence of a behavior analogous to the one described by the Balazs model, our observations also support the conclusions of a computational model by Chang, in which a state diagram was developed to predict the adhesive interactions between leukocytes and surfaces expressing selectin molecules.[35] In the state diagram, the rolling behavior of cells is divided into five distinct states. Each state is characterized by a unique profile of displacement versus time and is determined by the rate of shear, density of ligand−receptor pairs, dissociation rate, and bond interaction length. In addition to "firm adhesion" and "no adhesion", there exist three unique states of rolling adhesion, termed "fast adhesion", "transient adhesion", and "saltation". Over the range of shear rates tested by Chang (30−400 s^{-1}), cell rolling only occurred within a particular region of the state diagram, demonstrating that leukocyte rolling requires a delicate balance between ligand density, shear stress, and dissociation rate.

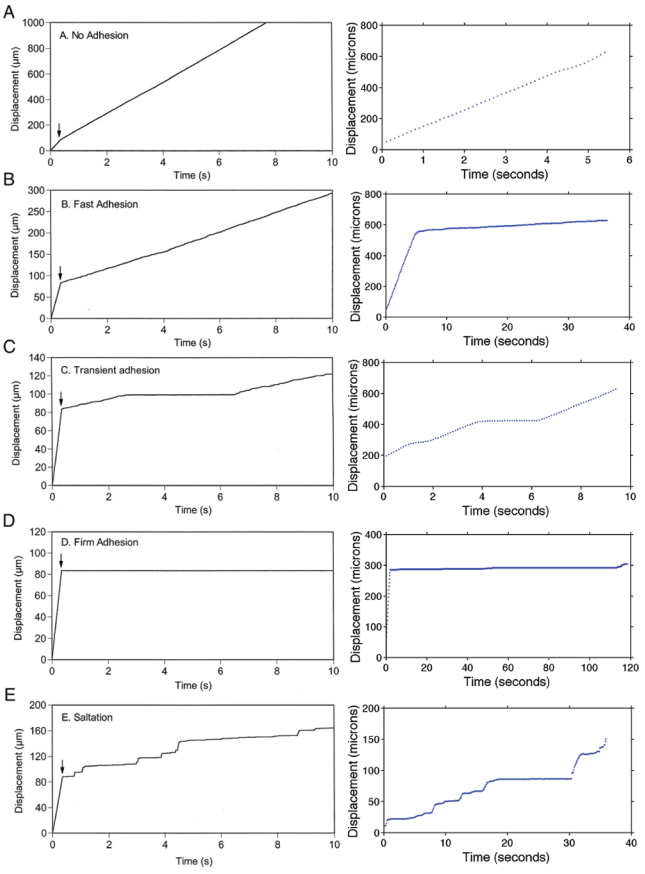

Figure 6. Plots of displacement versus time for the five states of adhesion identified by Chang (left) and sample plots of similar behavior identified in our cell tracking videos (right).[35] The five states are *no adhesion* (a), *fast adhesion* (b), *transient adhesion* (c), *firm adhesion* (d), and *saltation* (e). These behaviors represent different dynamic states of adhesion mediated by the biophysical and kinetic properties of the system. Left figure copyright (2000) National Academy of Sciences, U.S.A.

We were able to identify representative paths for each state of adhesion, the profiles of which are shown next to their corresponding graphs from Chang (Figure 6). These graphs represent the entire tracked path of a cell, and were not cropped to show only a portion of the path. The existence of all five states indicates that our experiments successfully captured a wide range of potential leukocyte behaviors within our shear stress range (0.29−2.2 dyn/cm^2). However, we were also able to observe more than one state of adhesion within each set of experimental parameters, indicating a considerable variability in the factors described above. The agreement between our observed data and the model proposed by Chang support the view that our cytotactic surface promotes leukocyte rolling.

In 2008, Karnik et al. observed the interaction of rolling HL-60 cells with a single patterned edge of P-selectin and a PEG-based blocking agent.[27] They found that rolling HL-60 cells were displaced orthogonal to the direction of flow when P-selectin edges were patterned at appropriate angles. A continuation of the 2008 study by the Karnik group recently suggested that patterned stripes may provide a label-free method of continuous cell separation.[28] The study was conducted under similar shear rates and P-selectin concentrations, but with larger stripe and chamber geometry, and at lower angles (≤20°). Karnik also used

dx.doi.org/10.1021/la203382k |*Langmuir* XXXX, XXX, 000–000

microcontact printing instead of covalent immobilization for P-selectin patterning. It was found that cell detachment was a random, history independent event, and that the rolling length could be modeled as a Poisson process. Additionally, Karnik found that edge inclination angle had a larger effect on cell displacement than P-selectin concentration (at low shear rates). Based on the displacements achieved, they predicted that a device on the length scale of 1 cm would be sufficient to sort a heterogeneous mixture of cells.[28] The study, however, did not utilize an experimental setup that was capable of sorting cells (GlycoTech parallel flow chambers, with only a single inlet and outlet, were used). Additionally, the fraction of cells interacting with the surface in their system was not reported. The microfluidic device that we describe herein will enable many of the limitations of first generation devices to be overcome. When our data are viewed at low resolution, our results parallel many of the findings from Lee and Karnik that show that patterned cytotactic surfaces displace the paths of rolling cells.

CONCLUSION

In conclusion, we have demonstrated the ability of smart surfaces to instruct specific behaviors in cell populations. The behaviors observed under these experimental conditions supported the predictions of two independent models of ligand binding and patterned surface interaction, including the Balazs model, which had not been previously validated with in vitro experimentation. This is important since the model also makes predictions about the sorting of cells on mechanically patterned surfaces, on which there have as yet been no experimental studies. By validating the predictions of this effect on chemically patterned surfaces, we have demonstrated the validity of the model and thus demonstrated its utility as a predictive tool. Hence, researchers can reliably use these predictions as guidelines for carrying out completely new experiments using mechanically patterned surfaces.

Because the motion of cells within our device can be predicted computationally, we are also in a position to rationally design improvements to the system, including physical and chemical changes to reduce permanent adhesions and increase the probability of cytotactic interactions. Presently the low rate of cytotactic interactions (<20%) is a limiting factor to the translation of this technique to practical application, but optimization of the channel geometry could yield significant improvements in efficiency. Reducing the channel height, recirculating unsorted cells, or introducing areas of turbulent flow to redistribute cells within the flow profile could all yield dramatic improvements in cell−surface interactions.

The ability to direct cell motion within a microfluidic device is an important tool for advanced diagnostics and experimental methods. The patterned substrate evaluated herein represents a new addition to those existing methods of cell control and is unique in its advantages and capabilities. The facile, label-free identification of specific cell types could lead to a myriad of advances in laboratory and clinical techniques that require fast, inexpensive cell purification.

ASSOCIATED CONTENT

Supporting Information. Additional images and videos. This includes images of the Balazs model, flow chamber, chemical procedure, and experimental setup, as well as a 3D rendition of the flow chamber and a sample experimental video. This material is available free of charge via the Internet at http://pubs.acs.org.

AUTHOR INFORMATION

Corresponding Author

*Mailing address: McGowan Institute for Regenerative Medicine, 450 Technology Drive, Suite 300, Pittsburgh, PA 15219. E-mail: russellaj@upmc.edu.

ACKNOWLEDGMENT

This project was funded by a grant from the Pennsylvania Department of Health and Pittsburgh Tissue Engineering Initiative (SAP#4100056872) and a grant from the Ethel Charitable Trust. In addition, ACB gratefully acknowledges funding from the DOE.

REFERENCES

(1) Bonner, W. A.; Hulett, H. R.; Sweet, R. G.; Herzenberg, L. A. *Rev. Sci. Instrum.* **1972**, *43*, 404.
(2) Herzenberg, L. A.; Parks, D.; Sahaf, B.; Perez, O.; Roederer, M.; Herzenberg, L. A. *Clinical Chemistry* **2002**, *48*, 1819.
(3) Bauer, J. *J. Chromatogr. B* **1999**, *722*, 55.
(4) Li, Y.; Dalton, C.; Crabtree, H. J.; Nilsson, G.; Kaler, K. V. I. S. *Lab Chip* **2007**, 239.
(5) Tsutsui, H.; Ho, C.-M. *Mech. Res. Commun.* **2009**, *36*, 92.
(6) Petersson, F.; Aberg, L.; Sward-Nilsson, A.-M.; Laurell, T. *Anal. Chem.* **2007**, *79*, 5117.
(7) MacDonald, M. P.; Spalding, G. C.; Dholakia, K. *Nature* **2003**, *426*, 421.
(8) Wang, M. M.; Tu, E.; Raymond, D. E.; Yang, J. M.; Zhang, H.; Hagen, N.; Dees, B.; Mercer, E. M.; Forster, A. H.; Kariv, I.; Marchand, P. J.; Butler, W. F. *Nat. Biotechnol.* **2004**, *23*, 83.
(9) Emmelkamp, J.; Wolbers, F.; Andersson, H.; DaCosta, R. S.; Wilson, B. C.; Vermes, I.; van den Berg, A. *Electrophoresis* **2004**, *25*, 3740.
(10) Norman, K. E.; Moore, K. L.; McEver, R. P.; Ley, K. *Blood* **1995**, *86*, 4417.
(11) Lawrence, M. B.; Springer, T. A. *Cell* **1991**, *65*, 859.
(12) Lawrence, M. B.; Kansas, G. S.; Kunkel, E. J.; Ley, K. *J. Cell Biol.* **1997**, *136*, 717.
(13) Alon, R.; Hammer, D. A.; Springer, T. A. *Nature* **1995**, *374*, 539.
(14) Burns, A. R.; Bowden, R. A.; Abe, Y.; Walker, D. C.; Simon, S. I.; Entman, M. L.; Smith, C. W. *J. Leukocyte Biol.* **1999**, *65*, 299.
(15) Chen, S.; Alon, R.; Fuhlbrigge, R. C.; Springer, T. A. *Proc. Natl. Acad. Sci. U.S.A.* **1997**, *94*, 3172.
(16) Davenpeck, K. L.; Brummet, M. E.; Hudson, S. A.; Mayer, R. J.; Bochner, B. S. *J. Immunol.* **2000**, *165*, 2764.
(17) Greenberg, A. W.; Kerr, W. G.; Hammer, D. A. *Blood* **2000**, *95*, 478.
(18) Hicks, A. E. R. *Blood* **2002**, *101*, 3249.
(19) Hong, S.; Lee, D.; Zhang, H.; Zhang, J. Q.; Resvick, J. N.; Khademhosseini, A.; King, M. R.; Langer, R.; Karp, J. M. *Langmuir* **2007**, *23*, 12261.
(20) Lasky, L. A. *Annu. Rev. Biochem.* **1995**, *64*, 113.
(21) Lorant, D. E.; McEver, R. P.; McIntyre, T. M.; Moore, K. L.; Prescott, S. M.; ZImmerman, G. A. *J. Clin. Invest.* **1995**, *96*, 171.
(22) Mayadas, T. N.; Johnso, R. C.; Rayburn, H.; Hynes, R. O.; Wagner, D. D. *Cell* **1993**, *74*, 541.
(23) Narasipura, S. D.; Wojciechowski, J. C.; Charles, N.; Liesveld, J. L.; King, M. R. *Clin. Chem.* **2007**, *54*, 77.
(24) Greenberg, A. W.; Hammer, D. A. *Biotechnol. Bioeng.* **2000**, *73*, 111.
(25) Chang, W. C.; Lee, L. P.; Liepmann, D. *Lab Chip* **2005**, *5*, 64.
(26) Alexeev, A.; Verberg, R.; Balazs, A. C. *Langmuir* **2007**, *23*, 983.

(27) Karnik, R.; Hong, S.; Zhang, H.; Mei, Y.; Anderson, D. G.; Karp, J. M.; Langer, R. *Nano Lett.* **2008**, *8*, 1153.
(28) Lee, C.-H.; Bose, S.; Van Vliet, K. J.; Karp, J. M.; Karnik, R. *Langmuir* **2011**, *27*, 240.
(29) Dong, C.; Lei, X. X. *J. Biomech.* **2000**, *33*, 35.
(30) Wu, L.; Xiao, B.; Jia, X.; Zhang, Y.; Lu, S.; Chen, J.; Long, M. *J. Biol. Chem.* **2007**, *282*, 9846.
(31) Patel, N.; Davies, M. C.; Hartshorne, M.; Heaton, R. J.; Roberts, C. J.; Tendler, S. J. B.; Williams, P. M. *Langmuir* **1997**, *13*, 6485.
(32) Bhattacharya, S.; Datta, A.; Berg, J. M.; Gangopadhyay, S. *J. Microelectromech. Syst.* **2005**, *14*, 590.
(33) Millare, B.; Thomas, M.; Ferreira, A.; Xu, H.; Holesinger, M.; Vullev, V. I. *Langmuir* **2008**, *24*, 13218.
(34) Gaver, D. P.; Kute, S. M. *Biophys. J.* **1998**, *75*, 721.
(35) Chang, K. C. *Proc. Natl. Acad. Sci. U.S.A.* **2000**, *97*, 11262.